REPORT DOCUMENTATION PAGE

Form Approved OMB NO. 0704-0188

1. REPORT DATE (DD-MM-YYYY)	2. REPORT TYPE	3. DATES COVERED (From - To)
04-07-2016	Final Report	1-Apr-2009 - 31-Mar-2016

4. TITLE AND SUBTITLE

Final Report: Characterization of nanoporous as a medium for size-selective filtration, preconcentration, and detection of biomolecules

5a. CONTRACT NUMBER
W911NF-09-1-0101

5b. GRANT NUMBER

5c. PROGRAM ELEMENT NUMBER
611102

6. AUTHORS
Sharon M. Weiss

5d. PROJECT NUMBER

5e. TASK NUMBER

5f. WORK UNIT NUMBER

7. PERFORMING ORGANIZATION NAMES AND ADDRESSES
Vanderbilt University
1400 18th Avenue South

Nashville, TN 37212 -2809

8. PERFORMING ORGANIZATION REPORT NUMBER

9. SPONSORING/MONITORING AGENCY NAME(S) AND ADDRESS (ES)

U.S. Army Research Office
P.O. Box 12211
Research Triangle Park, NC 27709-2211

10. SPONSOR/MONITOR'S ACRONYM(S)
ARO

11. SPONSOR/MONITOR'S REPORT NUMBER(S)
54322-CH-PCS.42

12. DISTRIBUTION AVAILIBILITY STATEMENT

Approved for Public Release; Distribution Unlimited

13. SUPPLEMENTARY NOTES

The views, opinions and/or findings contained in this report are those of the author(s) and should not contrued as an official Department of the Army position, policy or decision, unless so designated by other documentation.

14. ABSTRACT

This final report summarizes the accomplishments of W911NF-09-1-0101. In particular, the following significant advances were made: (1) improved understanding and quantification of diffusion coefficients and adsorption rates of various small molecules in nanoscale porous silicon; (2) invention of straightforward nanoscale patterning technique for porous materials (patent pending); (3) demonstration of dual mode sensing platform in porous silicon; (4) first demonstration of aptasensing in nanoscale porous media and aptamer-based detection of a toxin in porous silicon; (5) demonstration of cost-effective surface enhanced Raman scattering substrate based on patterned

15. SUBJECT TERMS

Final Report W911NF-09-1-0101

16. SECURITY CLASSIFICATION OF:			17. LIMITATION OF ABSTRACT	15. NUMBER OF PAGES	19a. NAME OF RESPONSIBLE PERSON
a. REPORT	b. ABSTRACT	c. THIS PAGE			Sharon Weiss
UU	UU	UU	UU		19b. TELEPHONE NUMBER 615-343-8311

Report Title

Final Report: Characterization of nanoporous as a medium for size-selective filtration, preconcentration, and detection of biomolecules

ABSTRACT

This final report summarizes the accomplishments of W911NF-09-1-0101. In particular, the following significant advances were made: (1) improved understanding and quantification of diffusion coefficients and adsorption rates of various small molecules in nanoscale porous silicon; (2) invention of straightforward nanoscale patterning technique for porous materials (patent pending); (3) demonstration of dual mode sensing platform in porous silicon; (4) first demonstration of aptasensing in nanoscale porous media and aptamer-based detection of a toxin in porous silicon; (5) demonstration of cost-effective surface enhanced Raman scattering substrate based on patterned nanoporous gold with robust understanding of enhancement mechanisms (patent pending); (6) advanced characterization of the corrosion of porous silicon upon exposure to negatively charged species; (7) first demonstration of simultaneous detection of small and large molecules using a new porous silicon Bloch surface wave sensor; (8) comprehensive characterization and demonstration of quantum dots as signal amplifiers in porous silicon sensors; (9) demonstration of sensing capability of nano- and micro-structured silicon optical structures that hold great promise for integrated sensor arrays with high detection sensitivity; and (10) fabrication of robust porous silicon membranes that allow evaluation of infiltration and binding kindetics in open-ended porous media.

Enter List of papers submitted or published that acknowledge ARO support from the start of the project to the date of this printing. List the papers, including journal references, in the following categories:

(a) Papers published in peer-reviewed journals (N/A for none)

Received		Paper
01/11/2011	3.00	Yang Jiao, Dmitry S. Koktysh, Nsoki Phambu, Sharon M. Weiss. Dual-mode sensing platform based on colloidal gold functionalized porous silicon, Applied Physics Letters, (10 2010): . doi:
01/11/2011	2.00	J. E. Sipe, J. D. Ryckman, S. M. Weiss, and M. Liscidini. Enhancement of diffraction-based biosensing using porous structures and electromagnetic surface states, Proceedings of SPIE, (01 2010): . doi:
02/13/2013	18.00	Jay G. Forsythe, Joshua A. Broussard, Jenifer L. Lawrie, Michal Kliman, Yang Jiao, Sharon M. Weiss, Donna J. Webb, John A. McLean. Semitransparent Nanostructured Films for Imaging Mass Spectrometry and Optical Microscopy, Analytical Chemistry, (12 2012): 10665. doi: 10.1021/ac3022967
04/29/2010	1.00	J. D. Ryckman, M. Liscidini, J. E. Sipe, and S. M. Weiss. Porous silicon structures for low-cost diffraction-based biosensing, Applied Physics Letters, (01 2010): . doi:
08/27/2015	36.00	Gilberto A. Rodriguez, Shuren Hu, Sharon M. Weiss. Porous silicon ring resonator for compact, high sensitivity biosensing applications, Optics Express, (03 2015): 7111. doi: 10.1364/OE.23.007111
08/28/2014	28.00	Sharon M. Weiss, Craig L. Duvall, Kelsey R. Beavers, Jeremy W. Mares, Caleb M. Swartz, Yiliang Zhao. In Situ Synthesis of Peptide Nucleic Acids in Porous Silicon for Drug Delivery and Biosensing, Bioconjugate Chemistry, (07 2014): 1192. doi: 10.1021/bc5001092
08/28/2014	32.00	Landon Oakes, Andrew Westover, Jeremy W. Mares, Shahana Chatterjee, William R. Erwin, Rizia Bardhan, Sharon M. Weiss, Cary L. Pint. Surface engineered porous silicon for stable, high performance electrochemical supercapacitors, Scientific Reports, (10 2013): 3020. doi: 10.1038/srep03020
08/28/2014	31.00	Gilberto A. Rodriguez, Judson D. Ryckman, Yang Jiao, Sharon M. Weiss. A size selective porous silicon grating-coupled Bloch surface and sub-surface wave biosensor, Biosensors and Bioelectronics, (03 2014): 486. doi: 10.1016/j.bios.2013.10.028
08/28/2014	30.00	Gilberto A Rodriguez, John D Lonai, Raymond L Mernaugh, Sharon M Weiss. Porous silicon Bloch surface and sub-surface wave structure for simultaneous detection of small and large molecules, Nanoscale Research Letters, (08 2014): 383. doi: 10.1186/1556-276X-9-383
08/28/2014	29.00	Yiliang Zhao, Jenifer L. Lawrie, Kelsey R. Beavers, Paul E. Laibinis, Sharon M. Weiss. Effect of DNA-Induced Corrosion on Passivated Porous Silicon Biosensors, ACS Applied Materials & Interfaces, (08 2014): 13510. doi: 10.1021/am502582s
08/31/2011	6.00	Xing Wei, Sharon M. Weiss. Guided mode biosensor based on grating coupled porous silicon waveguide, Optics Express, (05 2011): 11330. doi: 10.1364/OE.19.011330
08/31/2011	9.00	Judson D Ryckman, Peter N Ciesielski, Carlos A Escobar, G Kane Jennings, Yang Jiao, Sharon M Weiss. Patterned nanoporous gold as an effective SERS template, Nanotechnology, (07 2011): 295302. doi: 10.1088/0957-4484/22/29/295302

08/31/2011	8.00	Yang Jiao, Dmitry S. Koktysh, Nsoki Phambu, Sharon M. Weiss. Dual-mode sensing platform based on colloidal gold functionalized porous silicon, Applied Physics Letters, (10 2010): 153125. doi: 10.1063/1.3503608
08/31/2011	7.00	Judson D. Ryckman, Marco Liscidini, J. E. Sipe, S. M. Weiss. Direct Imprinting of Porous Substrates: A Rapid and Low-Cost Approach for Patterning Porous Nanomaterials, Nano Letters, (05 2011): 1857. doi: 10.1021/nl1028073
08/31/2013	20.00	Girija Gaur, Dmitry S. Koktysh, Sharon M. Weiss. Immobilization of Quantum Dots in Nanostructured Porous Silicon Films: Characterizations and Signal Amplification for Dual-Mode Optical Biosensing, Advanced Functional Materials, (08 2013): 3604. doi: 10.1002/adfm.201202697
08/31/2013	21.00	Yang Jiao, Judson D. Ryckman, Dmitry S. Koktysh, Sharon M. Weiss. Controlling surface enhanced Raman scattering using grating-type patterned nanoporous gold substrates, Optical Materials Express, (07 2013): 1137. doi: 10.1364/OME.3.001137
08/31/2013	22.00	Judson D. Ryckman, Yang Jiao, Sharon M. Weiss. Three-dimensional patterning and morphological control of porous nanomaterials by gray-scale direct imprinting, Scientific Reports, (03 2013): 1502. doi: 10.1038/srep01502
10/06/2012	14.00	Jeremy W. Mares, Sharon M. Weiss. Diffusion dynamics of small molecules from mesoporous silicon films by real-time optical interferometry, Applied Optics, (09 2011): 5329. doi: 10.1364/AO.50.005329
10/06/2012	15.00	Xing Wei, Jeremy W. Mares, Yandong Gao, Deyu Li, Sharon M. Weiss. Biomolecule kinetics measurements in flow cell integrated porous silicon waveguides, Biomedical Optics Express, (07 2012): 1993. doi: 10.1364/BOE.3.001993
TOTAL:	**19**	

Number of Papers published in peer-reviewed journals:

(b) Papers published in non-peer-reviewed journals (N/A for none)

Received	Paper
TOTAL:	

Number of Papers published in non peer-reviewed journals:

(c) Presentations

A. Simbula, G. A. Rodriguez, M. Menotti, M. Galli, D. Bajoni, S. M. Weiss, and M. Liscidini, "Four-wave mixing in porous silicon microring resonators," Conference on Lasers and Electro-Optics (CLEO), San Jose, CA, June 2016.

G. A. Rodriguez, M. Menotti, D. Aurelio, M. Liscidini, and S. M. Weiss, "Bloch surface wave ring resonators," Conference on Lasers and Electro-Optics (CLEO), San Jose, CA, June 2016.

S. M. Weiss, "Advanced photonic structures in porous silicon," 1st International Symposium on Functional Porous Materials, San Luis Potosí, Mexico, April 2016. (invited)

Y. Zhao, G. Gaur, T. Cao, P. E. Laibinis, and S. M. Weiss, "Flow-through porous silicon membranes for rapid, label-free biosensing," Porous Semiconductors – Science and Technology Conference, Tarragona, Spain, Mar. 2016. [Note: Y. Zhao received the Best Talk of the Day award for this presentation]

G. A. Rodriguez, A. P. Cartwright, P. Markov, and S. M. Weiss, "Advanced porous silicon photonic structures for biosensing applications," Porous Semiconductors – Science and Technology Conference, Tarragona, Spain, Mar. 2016.

S. M. Weiss, "Silicon photonics for sensing," Interdisciplinary Distinguished Seminar Series, North Carolina State University, Raleigh, NC, Oct. 2015. (invited)

K. J. Miller, G. A. Rodriguez, Y. Zhao, P. Markov, S. Hu, and S. M. Weiss, "Biosensing and optical modulation on a silicon platform," Center for Nanophase Materials Sciences Annual Users Meeting, Oak Ridge National Laboratory, Oak Ridge, TN, Sept. 2015.

S. M. Weiss, "Nanostructured silicon biosensors," SPIE Optics & Photonics, San Diego, CA, Aug. 2015. (invited)

Number of Presentations: 8.00

Non Peer-Reviewed Conference Proceeding publications (other than abstracts):

Received	Paper

TOTAL:

Number of Non Peer-Reviewed Conference Proceeding publications (other than abstracts):

Peer-Reviewed Conference Proceeding publications (other than abstracts):

Received	Paper
08/28/2014 34.00	Yiliang Zhao, Jenifer L. Lawrie, Paul E. Laibinis, Sharon M. Weiss. Understanding and mitigating DNA induced corrosion in porous silicon based biosensors, SPIE BiOS. 01-FEB-14, San Francisco, California, United States. : ,
08/31/2011 12.00	Yang Jiao, Dmitry S. Koktysh, Sharon M. Weiss. Dual Detection Platform with Refractive Index and SERS Sensing Based on Colloidal GoldFunctionalized Porous Silicon Substrates, Materials Research Society. 29-NOV-10, . : ,
08/31/2011 13.00	Xing Wei, Sharon M. Weiss. Grating coupled waveguide biosensor based on porous silicon, Materials Research Society. 29-NOV-10, . : ,
08/31/2013 23.00	Gilberto A. Rodriguez, Judson D. Ryckman, Yang Jiao, Robert L. Fuller, Sharon M. Weiss. Real-time detection of small and large molecules using a porous silicon grating-coupled Bloch surface wave label-free biosensor, SPIE BiOS. 02-FEB-13, San Francisco, California, USA. : ,
08/31/2013 24.00	Girija Gaur, Dmitry Koktysh, Sharon M. Weiss. Porous silicon biosensors using quantum dot signal amplifiers, SPIE BiOS. 06-FEB-13, San Francisco, California, USA. : ,
10/06/2012 16.00	J. W. Mares, X. Wei, S. M. Weiss. Porous materials for optical detection of chemicals, biological molecules, and high-energy radiation, Photonic Microdevices/Microstructures for Sensing IV. 26-APR-12, Baltimore, Maryland, USA. : ,
TOTAL:	**6**

Number of Peer-Reviewed Conference Proceeding publications (other than abstracts):

(d) Manuscripts

Received		Paper
01/11/2011	4.00	Judson D. Ryckman, Marco Liscidini, John E. Sipe, Sharon M. Weiss. Direct Imprinting of Porous Substrates: A Rapid and Low-Cost Approach for Patterning Porous Nanomaterials, Nano Letters (01 2011)
02/13/2013	19.00	Dmitry S. Koktysh, Sharon M. Weiss, Girija Gaur. Immobilization of Quantum Dots in Nanostructured Porous Silicon Films: Characterizations and Signal Amplification for Dual-Mode Optical Biosensing, Advaced Functional materials (09 2012)
08/31/2011	10.00	Jeremy W. Mares, Sharon M. Weiss. Diffusion dynamics of small molecules from mesoporous silicon films by real-time optical interferometry, Applied Optics (08 2011)
08/31/2013	25.00	Gilberto A. Rodriguez, Judson D. Ryckman, Yang Jiao, Sharon M. Weiss. A size selective porous silicon grating-coupled Bloch surface and sub-surface wave biosensor, Biosensors and Bioelectronics (07 2013)
TOTAL:		**4**

Number of Manuscripts:

Books

Received		Book
08/31/2011	11.00	J. L. Lawrie, S. M. Weiss. “Silicon photonics for biosensing applications,” in Silicon Photonics for Telecommunications and Biomedical Applications, in press: CRC Press, (10 2011)
TOTAL:		**1**

Received	Book Chapter
08/28/2014 33.00	J. L. Lawrie, S. M. Weiss, G. A. Rodriguez. "Nanoporous silicon biosensors for DNA sensing" in Porous Silicon for Biomedical Applications, Waltham, MA: Woodhead Publishing, (02 2014)
08/28/2015 37.00	Sharon M. Weiss, Shuren Hu. “Biological applications of silicon nanostructures,” in Silicon Nanophotonics: Basic Principles, Present Status, and Perspectives, 2nd edition, Hackensack: World Scientific Publishing Company, (01 2016)
TOTAL:	**2**

Patents Submitted

Patents Awarded

Awards

PI, Sharon Weiss, named IEEE Photonics Society Distinguished Lecturer (2016-2017)

PI, Sharon Weiss, awarded the Vanderbilt School of Engineering Excellence in Teaching Award (2015-2016 academic year)

Participating graduate student, Yiliang Zhao, awarded Best Talk of the Day at the Porous Semiconductors – Science and Technology Conference in Tarragona, Spain, in March 2016

Graduate Students

NAME	PERCENT_SUPPORTED	Discipline
Girija Gaur	0.27	
Gilberto Rodriguez	0.86	
Yiliang Zhao	0.90	
FTE Equivalent:	**2.03**	
Total Number:	**3**	

Names of Post Doctorates

NAME	PERCENT_SUPPORTED
FTE Equivalent:	
Total Number:	

Names of Faculty Supported

NAME	PERCENT_SUPPORTED	National Academy Member
Sharon Weiss	0.02	
Jeremy Mares	0.04	
FTE Equivalent:	**0.06**	
Total Number:	**2**	

Names of Under Graduate students supported

NAME	PERCENT_SUPPORTED	Discipline
Alyssa Cartwright	0.00	Electrical Engineering
FTE Equivalent:	**0.00**	
Total Number:	**1**	

Student Metrics

This section only applies to graduating undergraduates supported by this agreement in this reporting period

The number of undergraduates funded by this agreement who graduated during this period: 0.00

The number of undergraduates funded by this agreement who graduated during this period with a degree in science, mathematics, engineering, or technology fields:..... 0.00

The number of undergraduates funded by your agreement who graduated during this period and will continue to pursue a graduate or Ph.D. degree in science, mathematics, engineering, or technology fields:..... 0.00

Number of graduating undergraduates who achieved a 3.5 GPA to 4.0 (4.0 max scale):..... 0.00

Number of graduating undergraduates funded by a DoD funded Center of Excellence grant for Education, Research and Engineering:..... 0.00

The number of undergraduates funded by your agreement who graduated during this period and intend to work for the Department of Defense 0.00

The number of undergraduates funded by your agreement who graduated during this period and will receive scholarships or fellowships for further studies in science, mathematics, engineering or technology fields: 0.00

Names of Personnel receiving masters degrees

NAME
Total Number:

Names of personnel receiving PHDs

NAME
Girija Gaur
Gilberto Rodriguez
Total Number: 2

Names of other research staff

NAME	PERCENT_SUPPORTED
FTE Equivalent:	
Total Number:	

Sub Contractors (DD882)

Inventions (DD882)

Scientific Progress

See Attachment

Technology Transfer

Final licensing negotiations are being conducted for S. M. Weiss, Y. Jiao, J. D. Ryckman, P. N. Ciesielski, G. K. Jennings, “Nanoscale porous gold film SERS template,” U.S. Patent Application Number 13/825,152 and S. M. Weiss, J. D. Ryckman, M. Liscidini, and J. E. Sipe, “Direct imprinting of porous substrates,” U.S. Patent Application Number 12/790,908.

FINAL REPORT: Scientific Progress and Accomplishments

ARO W911-NF-09-1-0101: *Characterization of Nanoporous Silicon as a Medium for Size-Selective Filtration, Preconcentration, and Detection of Biomolecules*

PI: Sharon M. Weiss, Vanderbilt Unversity

The primary goal of this project was to advance the state of knowledge at the bio-nano interface of nanoporous materials. A multitude of significant accomplishments resulted from this project, as described by scientific publication and presentations, as well as through earlier progress reports. In this document, several key highlights are discussed.

(1) Improved understanding and quantification of diffusion coefficients and adsorption rates of various small molecules in nanoscale porous silicon

Porous materials have been shown to exhibit several advantageous characteristics for sensing applications. Nanoscale pores offer enormous internal surface area that is available for molecular binding. Moreover, pores enable size-exclusion capabilities that minimize contamination from larger particles in complex media. One potential concern for sensors based on nanoscale porous materials is the response time since it may take molecules longer to diffuse into and attach within a nanoscale pore compared to a flat surface. Hence, we studied the molecular binding kinetics and diffusion dynamics of small molecules in nanoscale porous silicon. At the end of the project, we also were able to form porous silicon membrane structure to begin to carry out a comparative study of the kinetics in open-ended versus closed-ended pores (see section 10).

In order to quantitatively determine the kinetics parameters of several kinds of biomolecules in closed-ended porous silicon, we performed real-time monitoring of biomolecule attachment events in grating-coupled porous silicon waveguide biosensors. An illustration of the porous silicon waveguides and their sensor operation is shown in Fig. 1 [1-3]. We designed and fabricated a PDMS flow cell on top of the waveguide to control the flow of molecules into the waveguide. Time-dependent reflectance measurements were carried out to elucidate the binding kinetics [1]. Light incident on the grating is coupled into the waveguide at a specific angle that depends on the wavelength of light and the optical thickness of the porous silicon waveguide. When molecules bind within the porous silicon waveguide, the effective index and, correspondingly, the optical thickness of the waveguide change, causing the angle at which light is coupled into and out of the porous silicon waveguide to change. The angular shift of the diffracted light can be directly correlated with the quantity of molecules attached within the waveguide. Our real-time measurement approach along with computations based on mass balance equations allow us to additionally extract the rates at which these molecules infiltrate and attach in the nanoscale pores [1]. Kinetic parameters of small chemical molecules and nucleic acid molecules were determined. Figure 2 shows the

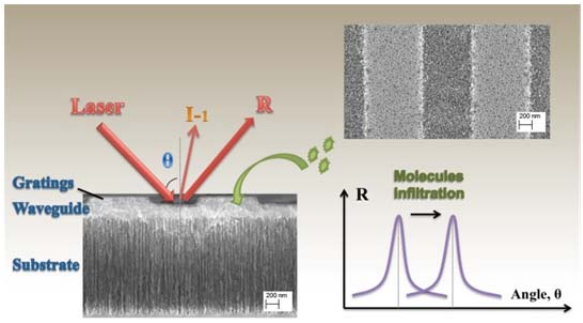

Figure 1. (bottom left) Cross-sectional SEM image of porous silicon waveguide with porous silicon grating coupler, and illustration of optical interrogation of the sensor. (upper right) Plan view SEM of the porous silicon grating. (bottom right) Example reflectance spectra showing waveguide resonance shift after infiltration of molecular species into the porous silicon waveguide.

experimental results of the dynamic process of the infiltration and attachment of all the chemical and biological molecules. The effects of both volume infiltration and molecular surface attachment on the waveguide resonance angle can be observed. The effect of volume infiltration (e.g., molecular infiltration into the pores without surface attachment) is shown by the immediate and dramatic change in reflectance after solution injection. Molecular attachments are confirmed by the residual resonance angle shifts measured after the rinsing step that follows each molecular infiltration. In the data set presented, the functionalized porous silicon waveguide was first exposed to a mismatched PNA sequence before introducing the complementary PNA target sequence to demonstrate the selectivity of the sensing system. Based on the results of our experiments, we anticipate at least 5:1 selectivity of the sensor to complementary target sequences. In order to analyze adsorption kinetics in porous silicon, we used a two-dimensional diffusion model that takes into account mass transportation and binding reactions between molecules in bulk solution and immobilized groups at the pore walls. Complete details can be found in Ref. [1]. A summary of the ascertained diffusion coefficients, adsorption rate constants, and desorption rate constants are shown in Table 1. In porous media, the diffusion coefficient is affected by the morphology of the porous material and is lower than the free solution diffusion coefficient because of the constricted, elongated or tortuous solute flow paths. We note that for the larger oligos, the diffusion coefficient in porous silicon is nearly 10-fold smaller than that in free solution. We further note that the adsorption rate constant of the molecules is 10^2-10^4 times smaller than that on flat surfaces due to the nanoscale confined geometry that exists in the pores. Nevertheless, since Fig. 2 shows that the resonance shift saturates within a few to several minutes, and the total measured resonance shift is several times larger than the limit of detection, porous silicon sensors are capable of reporting diagnostic outcomes on near real-time scales.

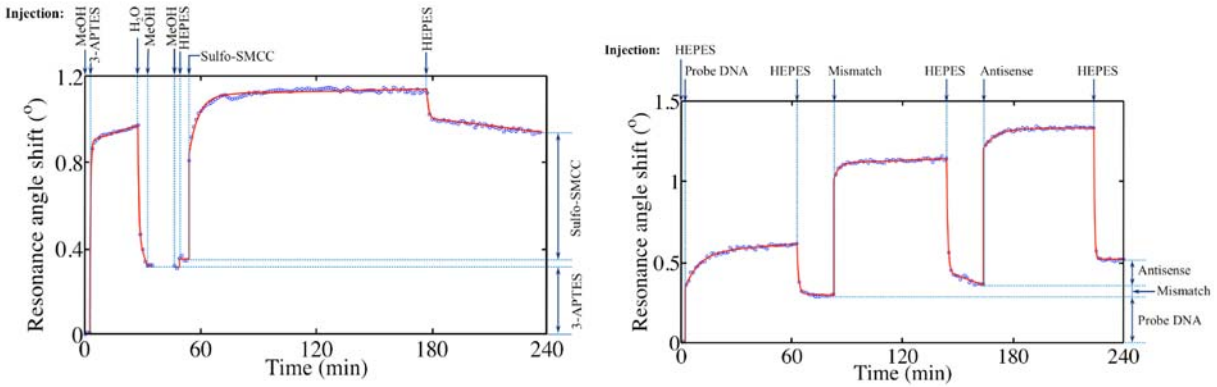

Figure 2. (a) Resonance angle shift during 3-APTES and Sulfo-SMCC attachments at room temperature. The gap between two curves (35–45 min) is for the 3-APTES annealing process. (b) Resonance angle shift during exposure to probe DNA, mismatch PNA, and antisense PNA, performed at 37°C. In both graphs, blues circles are experimental data and the fitted curves are shown for visual guidance. All molecular species are specified in Table 1. [1]

Table 1. Diffusion coefficient, adsorption and desorption rate constants of various small molecules in porous silicon: 3-aminopropyltriethoxysilane (3-APTES, 4%), sulfosuccinimidyl 4-[N-maleimidomethyl] cyclohexane-1-carboxylate (Sulfo-SMCC, 2.5mg·L^{-1}), 16-base thiol modified probe DNA (5′-TAG CTA TGG TCC TCG T-3′, 3′ Thiol C3), complementary peptide nucleic acid (PNA, ACG AGG ACC ATA GCT A). [1]

	3-APTES	Sulfo-SMCC	Probe DNA	Antisense PNA
D ($m^2 \cdot s^{-1}$)	5.41×10^{-9}	2.442×10^{-9}	9.542×10^{-11}	9.576×10^{-11}
k_{ad} ($M^{-1} \cdot s^{-1}$)	0.02958	0.1274	5.641	4.442
k_{des}(s^{-1})	7.652×10^{-5}	1.748×10^{-5}	7.4×10^{-6}	1.422×10^{-5}

Enhanced understanding of the diffusion dynamics of molecular species in nanoscale porous materials as compared to bulk solution was achieved through the development of a time-dependent laser reflectometry measurement scheme and a modified Fickian diffusion flow model [5]. A custom-made diffusion apparatus was utilized for the time-dependent optical reflectometry measurements, as illustrated in Fig. 3a. The diffusion apparatus consists of two chambers separated by a gate. One chamber holds an ambient liquid medium and the other chamber holds the solution containing the molecules of interest. The porous material can be submerged in either solution to determine the diffusion dynamics of molecules into or out of the pores. Diffusion dynamics in porous silicon films were determined using sucrose as the model molecule and an ambient medium of water. The porous silicon sample was initially loaded with the sucrose solution. When the gate was opened, sucrose diffusion was monitored to determine the diffusion dynamics of the small molecules out of the nanoscale pores. Optical reflectometry measurements were conducted by aligning laser light to be incident on the porous silicon sample surface through the front chamber of the diffusion apparatus and then monitoring the intensity of the reflected beam over time. Diffusion coefficients were calculated by applying a modified Fickian diffusion flow model to the measured time-dependent reflectance data [5]. A summary of the measured time-dependent change in reflectance and calculated diffusion coefficients for nanoscale porous silicon films with an average pore diameter between 10-30 nm and a thickness between 300-900 nm is shown in Fig. 4(b,c). We found that the time duration necessary to reach signal steady-state increases with increasing film thickness, as expected. The calculated diffusion coefficients correspondingly increase with decreasing film thickness and were also found to increase with increasing pore size. Thus, the diffusion coefficient of the thinnest and largest pore size films approach, and become approximately equal to, the bulk diffusion coefficient for sucrose in water. This trend is explained by considering that diffusion is hindered by interactions of the molecules with the pore walls, which are essentially scattering events. Hence, a molecule diffusing out of a thicker film will have more opportunity to interact with the pore walls, which slows the release rate. Our studies show that the diffusion coefficient of molecules in nanoscale porous silicon can be tuned by adjusting the pore size and film thickness. These results have been used to facilitate the design of sensors that best balance response time and sensitivity.

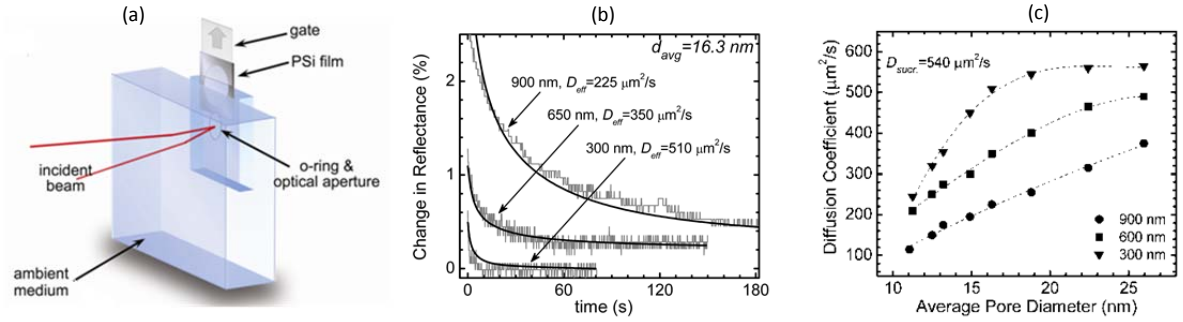

Figure 3. (a) Schematic of the diffusion chamber apparatus used for measurement of optical reflectance during diffusion experiments with porous silicon (PSi) films. (b) Change in reflectance during sucrose diffusion for three films of different thickness but equal mean pore diameter (16 nm). The modeled best-fit curve to the data (smooth) is shown for each curve along with the fitted effective diffusion coefficients. Note that the curves are shifted with respect to each other by 0.25% for image clarity. (c) Effective diffusion coefficients of porous silicon samples with varying thicknesses and average pore diameters. The diffusion coefficient of sucrose in water (at room temperature) is 540 $\mu m^2/s$. [5]

(2) Invention of straightforward nanoscale patterning technique for porous materials

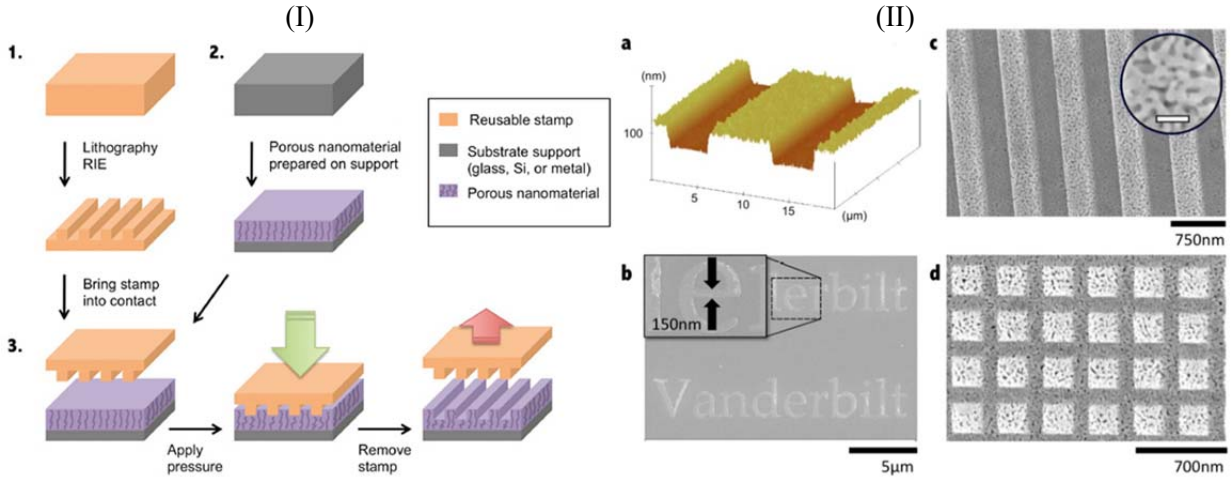

Figure 4. (I) Illustration of direct imprinting of porous substrates (DIPS) technique to pattern porous materials with nanoscale resolution. (1) A reusable stamp is patterned by standard lithography and reactive-ion-etching. (2) The porous material is prepared on a substrate (e.g. silicon, glass, or metal). (3) The stamp is then imprinted into the porous material with the desired force. (II) (a) Atomic force microscope image of porous silicon grating (Λ = 10μm). The mean pore diameter is ~20-30nm. (b-d) Plan view scanning electron microscope images of porous nanomaterials patterned with DIPS. (b) Porous silicon imprinted with 3μm font "Vanderbilt" text, showing the capability to imprint arbitrary shapes with feature sizes on the order of 100nm. (c) Nanoporous gold grating (Λ = 750nm). Inset reveals the original pore morphology (scale bar = 100nm). (d) Nanoporous gold square mesh (Λ = 350nm). [6]

While the fabrication of porous films is often very straightforward, for example requiring a simple anodization procedure, subsequent micro- and nanoscale patterning of these porous films

requires sophisticated methods such as electron beam lithography and reactive ion etching. We developed a technique for one-step, direct patterning of porous nanomaterials (including insulators, semiconductors, and metals) that does not require intermediate polymer processing or dry etching steps. Our process, which we call 'direct imprinting of porous substrates' (DIPS), utilizes reusable stamps with micro- and nanoscale features that are applied directly to a porous material to selectively compress or crush the porous network [6, 7]. As illustrated in Fig. 4, the stamp pattern is transferred to the porous material with high fidelity, vertical resolution below 5 nm, and lateral resolution below 100 nm. The process is performed in less than one minute at room temperature and at standard atmospheric pressure. Using the DIPS process, we fabricated and patented cost-effective and high performing porous silicon diffraction grating sensors (Fig. 3, IIa) [8] and patterned nanoporous gold surface enhanced Raman scattering substrates (described in section 5 and also shown in Fig. 4, IId) [9, 10].

(3) Demonstration of dual mode sensing platform in porous silicon

Sensors that support multiple functionalities provide the advantages of more robust sensor results with self-confirmation and a broader range of detectable analytes. We reported on the first hybrid porous silicon-gold nanoparticle structure that combines molecular quantification via reflectance measurements and molecule identification via surface enhanced Raman scattering (SERS) spectral analysis on a single substrate [4]. The dual mode sensor is fabricated by infiltrating colloidal gold nanoparticles into and on top of a porous silicon film (Fig. 5). Sensor performance was benchmarked with benzenethiol molecules. A spectral shift of the thin film interference fringes from the hybrid structure was measured in reflection upon benezenethiol attachment due to the benzenethiol molecule-induced overall refractive index change of the porous silicon film. This measurement confirmed and quantified the addition of molecules to the sensor. A detection sensitivity of ~400 nm/RIU was estimated. Next, distinct SERS peaks representative of the benzenethiol molecule were observed, most likely due to benzenethiol attachment to the dense distribution of Au NPs on the roughened surface of the porous silicon film. Good uniformity of the SERS signal across the sample was detected. This measurement provided unique molecular identification that complemented the quantification from the reflectance measurements.

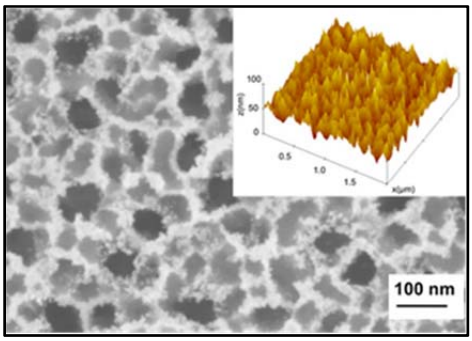

Figure 5. Top-view SEM image showing porous silicon film coated with small (~4.5 nm) colloidal gold nanoparticles for dual mode sensing. Inset shows an AFM image of the roughened porous silicon surface. [4]

(4) Demonstration of aptasensing in nanoscale porous media and aptamer-based detection of a toxin in porous silicon

We reported the first demonstration of aptamer bioreceptors in a nanoscale porous medium for selective molecular detection. Theoretically, a high affinity and highly selective aptamer

could be found for any desired target, given a large enough library of oligos to search, which is a significant advantage of aptamers compared with other bioreceptor classes, such as antibodies. We first showed aptasensing in porous silicon waveguides to capture the small molecule, adenosine, which has important applications in studies of cardiac ischemia [11]. The inset in Fig. 6a provides a schematic of the aptamer binding mechanism for adenosine. Two adenosine molecules are captured by the DNA aptamer, which changes its conformation in the presence of the target adenosine molecules. The aptamer sequence to capture adenosine (3'-TGG AAG GAG GCG TTA TGA GGG GGT CCA-5') was synthesized via the phosphoramidite method in a porous silicon film that was prefunctionalized with a hydroxyl terminated silane. Adenosine-containing buffer solution was dropped into the aptamer-functionalized porous silicon waveguide at 60°C, and incubation and subsequent rinsing steps were performed at 4°C. The measured change in the waveguide resonance angle directly correlated to the target solution concentration with a minimum detectable concentration of 10μM. This detection sensitivity is comparable to some of the most sensitive aptamer-based adenosine detection platforms previously reported, but is impressively achieved without the incorporation of labels or signal amplifiers. We also investigated a competitive displacement approach to detecting adenosine using a DNA aptamer partially hybridized with complementary 12mer DNA; adenosine capture by the aptamer releases the 12mer DNA producing a measurable reflectance shift [11]. Specificity of the target binding achieved with the adenosine aptamer as demonstrated using a porous silicon waveguide aptasensor incubated in a saturated target solution of uridine, a commonly used control molecule for adenosine sensors due to its size and structural similarities. Exposure to uridine did not result in a measurable resonance shift; thus, uridine was not bound by the aptamer. Furthermore, after exposure to the negative control uridine, aptamer functionalized samples were again exposed to adenosine, producing a shift in resonance angle and indicating that the aptamer maintains its functionality throughout the control experiments.

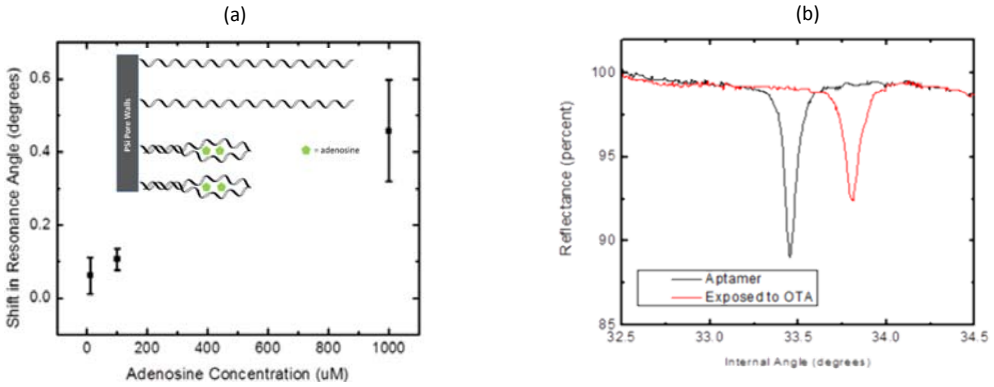

Figure 6. (a) Measured shift in porous silicon waveguide resonance angle upon exposure of aptamer-functionalized porous silicon waveguides to different concentrations of adenosine target. Inset shows aptamer binding mechanism for adenosine target. In the presence of adenosine, the ssDNA aptamer binds two adenosine target molecules. (b) Reflectance measurements showing target capture of 1μM OTA toxin in an aptamer-functionalized porous silicon waveguide. [11]

We next demonstrated the application of aptamers for the detection of Ochratoxin A (OTA) [11], a mycotoxin that is found as a contaminant in improperly stored food commodities. Preparation of the porous silicon sensor for OTA detection proceeded similar as to that reported for adensine detection with the exception that a different DNA apatamer sequence was required: 5'-GAT CGG GTG TGG GTG GCG TAA AGG GAG CAT CGG ACA-3'. Figure 6b shows the optical detection of OTA in phosphate buffered saline. Based on multiple measurements, we anticipate a detection limit at or below 100 nM using the porous silicon aptasensor, which is below the cut-off for many food categories to ensure safety of the feedstock.

(5) Demonstration of cost-effective surface enhanced Raman scattering substrate based on patterned nanoporous gold with robust understanding of enhancement mechanisms

We invented and subsequently characterized a new SERS platform based on patterned nanoporous gold (NPG) that is highly uniform, efficient, and cost-effective [9, 10]. Using the DIPS process described in section 2, subwavelength gratings were defined in a NPG film by densifying appropriate regions of the film. The NPG film itself was formed using a simple dealloying technique. The patterned NPG (P-NPG) structures are shown in Fig. 7a. The SERS enhancement from these structures results from a combination of localized surface plasmon and surface plasmon polariton effects. The closely arranged nanoscale gold ligaments that constitute NPG give rise to the localized surface plasmon-based enhancement and the patterned gratings give rise to the propagating surface plasmon-based enhancement. Careful investigations were conducted to understand how the design parameters of the grating (i.e., pitch, height, fill factor) and the NPG pore size affected the SERS enhancement factor. As shown in Fig. 7b, using benzenethiol as the SERS active molecule under test, our P-NPG template exhibits a SERS intensity that is several orders of magnitude stronger than unpatterned NPG and is at least one order of magnitude greater than the gold-standard, Klarite® substrate. We estimate the SERS enhancement to be near 10^8 [10].

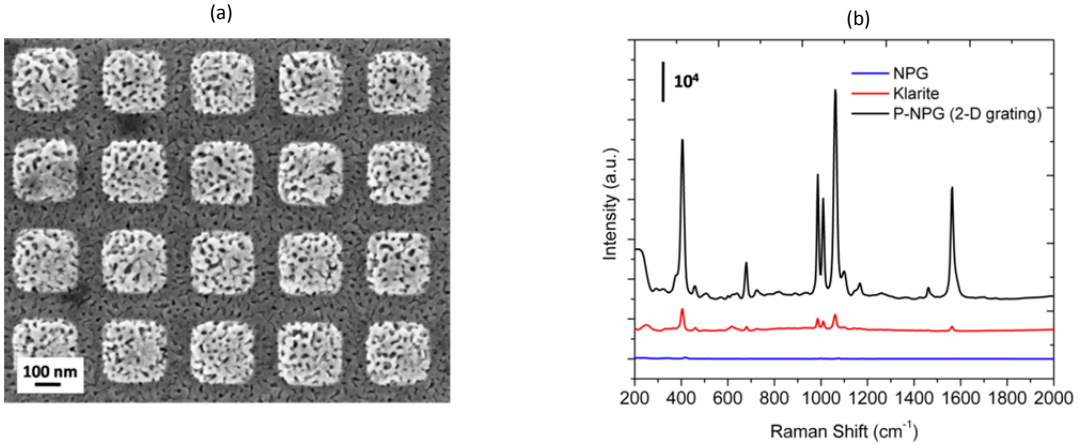

Figure 7. (a) Plan view SEM image of a representative surface morphology of a patterned nanoporous gold (P-NPG) SERS template. (b) SERS spectra of benzenethiol molecules adsorbed on NPG (blue), Klarite® commercial SERS substrate (red), and 2-D P-NPG SERS substrate with 650 nm pitch and air fill fraction of ~30% (black). The spectra are offset for ease of comparison. [9]

(6) Advanced characterization of the corrosion of porous silicon upon exposure to negatively charged species

A significant challenge for porous silicon sensors is the reactivity of the surface in certain environments. For example, it is well-known that unpassivated porous silicon will rapidly degrade in aqueous environments. What is less well understood, although empirically observed, is the oxidation and subsequent corrosion of porous silicon upon exposure to negatively charges species. This undesirable corrosion process severely limits the reliability, reusability, and sensitivity of porous silicon DNA sensors. We investigated methods to mitigate this corrosion effect and proposed a model to explain our empirical results [12, 13]. We believe that corrosion initiates at porous silicon surface regions with exposed Si-H or Si-OH bonds and is accelerated when the binding of negatively charged DNA results in the local accumulation of positive charge carriers from the silicon matrix, which polarizes the nearby Si-H or Si-OH bonds and facilitates nucleophilic attack by water molecules. We found that surface passivation plays a strong role in the corrosion process: pore surfaces that are well-passivated, for example with silicon dioxide and an amino-silane, are resilient against corrosion while regions that are not sufficiently passivated are susceptible to corrosion.

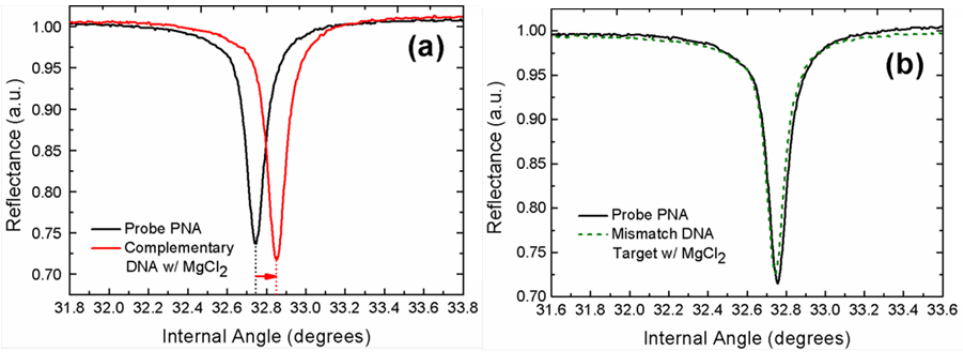

Figure 8. Functionalization of porous silicon waveguide surface with neutrally-charged PNA probes helps to mitigate waveguide corrosion during hybridization with DNA targets (i.e., red-shift due to hybridization instead of blue-shift due to corrosion). Addition of Mg^{2+} ions fully mitigates the porous silicon corrosion during hybridization of DNA targets to PNA probes. Resonance shifts are shown for a PNA functionalized porous silicon waveguide upon incubation with (a) 100% complementary DNA and (b) 100% mismatch DNA. [12]

Since it is challenging to achieve complete surface passivation with most functionalization approaches, we utilized two methods to mitigate the corrosion effect that rely on minimizing the effect of the negative charge [12]. First, instead of using DNA receptor molecules, neutrally charged PNA receptor molecules were employed [14]. PNA bases hybridize strongly to complementary target DNA bases but do not possess the negatively charged backbone. Hence, use of PNA receptor molecules eliminates corrosion associated with the binding of receptor molecules. In order to shield the porous silicon surface from the negative charges on the phosphate groups of the target DNA molecules, and to fully mitigate DNA-induced corrosion of

porous silicon, Mg^{2+} ions were introduced into the incubation solution used for target molecule hybridization. When binding to the DNA strands, Mg^{2+} ions can shield the negative charge accumulated at the porous silicon surface, which prevents porous silicon corrosion and enhances the detection signal for the PNA functionalized porous silicon waveguide. Figure 8a shows the resonance red-shift upon hybridization of a PNA functionalized porous silicon waveguide with 10 μM complementary target DNA molecules after 1 hour incubation. A negligible resonance shift was detected for mismatch DNA target in the same buffer solution with Mg^{2+}, suggesting there are no non-specific binding events (Fig. 8b). Passivated porous silicon waveguide biosensors can achieve a detection limit below 10 nM.

(7) Demonstration of simultaneous and size-selective detection of small and large molecules using a new porous silicon Bloch surface wave sensor

While porous silicon sensors have been demonstrated as an attractive label-free biosensing platform due to their highly tunable optical properties, enhanced surface area, and rapid and cost-effective fabrication, a key limitation facing these sensors is the ability to effectively detect large molecules that either slowly diffuse into or are filtered out by the pores. To overcome this challenge, we demonstrated a label-free method for size-selective sensing of both small (<2nm) and large (>10nm) low molecular weight molecules (<15 kDa) using a newly designed grating-coupled Bloch surface wave (BSW) and Bloch sub-surface wave (BSSW) porous silicon multilayer structure (SEM image shown in Fig. 9a) [15-17]. The BSW is an optical surface state that can be effectively employed for the detection of surface-bound molecules that are too large to infiltrate the porous matrix. The BSSW, first introduced by our group, is confined just beneath the surface and has a strong sensitivity to small molecules that penetrate the porous matrix [15]. The BSW is created by introducing a top layer in a porous silicon Bragg stack that has a reduced optical thickness. Introducing a second layer with a properly designed reduced optical thickness ("step index" design) leads to a single BSSW mode supported within the porous silicon multilayer film. Introducing a continuous gradient in the optical thickness of the multilayer porous silicon film instead ("gradient index" design) leads to multiple BSSW modes that can be supported. One of the important outcomes of this work is that we now have the ability to design strongly confined modes at nearly arbitrary depths within a nanoscale porous silicon film, enabling molecular size-dependent and infiltration depth dependent sensing. The porous silicon BSW/BSSW sensor platform has the capability to detect both large and small molecules (relative to the pore diameter, ≈ 20 nm) with high sensitivity (>2,000nm/RIU); this capability is not present in any other porous silicon sensor system. Fig. 9b demonstrates the capability of size-selective sensing through the detection of M13KO7 bacteriophage to a glutaraldehyde functionalized BSW/BSSW sensor: the BSW resonance shifts due to the presence of the surface bound bacteriophage while the BSSW resonance does not shift because the large molecule does not infiltrate the nanoscale pores where the BSSW mode is confined [16].

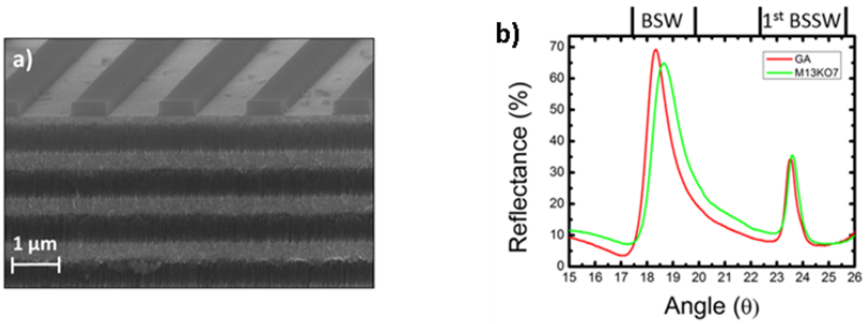

Figure 9. (a) SEM cross-sectional image of porous silicon BSW/BSSW sensor. (b) Measured reflectance spectra before and after the attachment of large M13KO7 bacteriophage to a glutaraldehyde (GA) functionalized BSW/BSSW sensor. Only the BSW mode resonance shifts, confirming the attachment of the large, surface-bound bacteriophage. [15, 16]

(8) Comprehensive characterization and demonstration of quantum dots as signal amplifiers in porous silicon sensors

In order to further enhance the detection capabilities of porous silicon-based biosensors, and to facilitate straightforward methods of multiplexed detection of multiple analytes, we demonstrated the use of colloidal quantum dots (QDs) as signal amplifiers [18]. QDs serve both as high refractive index signal amplifiers for optical reflectance measurements that can quantify the number of molecules captured and as fluorescent emitters whose distinct emission wavelength confirms molecule capture in the functionalized pores. To demonstrate this concept, target biotin molecules were conjugated with low-toxicity $AgInS_2/ZnS$ QDs and exposed to streptavidin-functionalized porous silicon films. Figure 10 shows the comparison of the porous silicon sensor detection of QD-biotin conjugates compared to unlabeled biotin targets. Along with the characteristic fluorescence signal, a 5-fold enhancement in the measured spectral

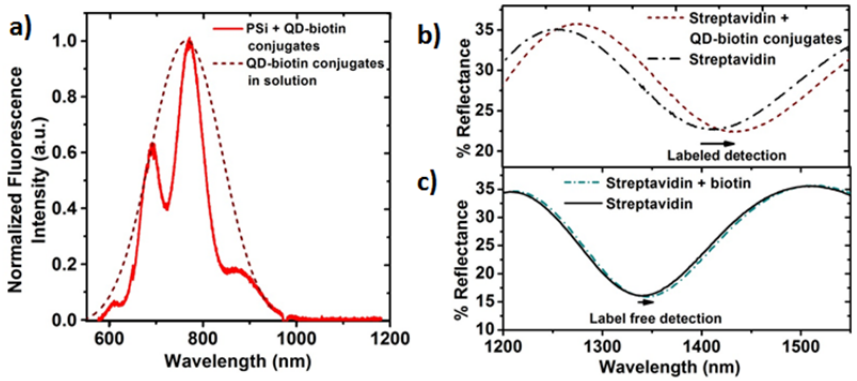

Figure 10. (a) Fluorescence spectra of QD-biotin conjugates in solution and bound inside a streptavidin-functionalized porous silicon (PSi) film. The fluorescence of the conjugates inside the film is modulated due to thin film interference effects and demonstrates that the conjugates are inside as opposed to only on top of the porous silicon film. Reflectance spectra for the detection of biotin (b) with and (c) without the use of QD-conjugates from two different porous silicon samples functionalized with streptavidin probes. Use of the QDs conjugated to biotin molecules significantly amplifies the sensor response. [18]

reflectance shift is observed, which results in a nearly three order of magnitude improvement in the detection limit from pg/mm^2 to fg/mm^2. These remarkable results were achieved with only 6% QD bioconjugate coverage in the pores; sub-fg/mm^2 detection limits should be readily achievable with this platform. Negligible non-specific binding was observed in control experiments. Choosing the appropriately sized QD for given pore sizes is important for achieving maximum sensitivity. A comprehensive characterization of mesoporous silicon films as a function of pore size, surface area, and QD coverage was reported in Ref. [18].

(9) Demonstration of sensing capability of porous silicon optical structures that hold great promise for integrated sensor arrays with high detection sensitivity

For sensor array configurations, in-plane optical coupling of light into porous silicon optical structures is advantageous so that sensor array elements can be aligned in tandem and the signal from multiple sensor elements can be encoded in a single transmission spectrum. We reported the first demonstration of a porous silicon ring resonator waveguide sensor that utilizes in-plane coupling. SEM images of our porous silicon ring resonator are shown in Fig. 11 [19]. The sensors are made by first fabricating planar porous silicon waveguides using conventional electrochemical etching and then using electron beam lithography and reactive ion etching to pattern the ring structure into the porous silicon surface guiding layer. Based on exposure to various salt water solutions, the bulk detection sensitivity of a porous silicon ring resonator was determined to be ≈ 450 nm/RIU, which represents a 3-fold increase in bulk detection sensitivity compared to nonporous silicon-on-insulator (SOI) ring resonators, such as those that have been commercialized. The molecular detection sensitivity of the porous silicon ring resonators was characterized by functionalization with a 16-base DNA molecule for the capture of a 16-base complimentary PNA molecule. Exposure of the porous silicon ring resonator to 500 nM target PNA solution resulted in a 2 nm resonance shift, leading to a remarkable sensitivity of 4 pm/nM, which is one order of magnitude greater than that reported for nucleic acid detection using SOI ring resonators. The improved detection sensitivity is due in large part to the enormous available sensing area of the porous silicon ring resonators where there is strong light-molecule interaction (as illustrated in Fig. 11d).

We also recently demonstrated porous silicon photonic crystal nanobeam sensors that share the same in-plane coupling advantage of the porous silicon ring resonators [20]. However, while the transmission spectra of ring resonators are characterized by multiple resonances, nanobeams possess only a single resonance. With multiple resonances, if molecular attachment in the porous silicon ring causes the resonance to shift by more than the spacing between adjacent resonaces, then it becomes difficult to determine the magnitude of the shift and quantitatively determine the analyte concentration unless the resonance position is continuously monitored. This potential measurement ambiguity is not present for the porous silicon nanobeam sensors. SEM images of the porous silicon nanobeam are shown in Fig. 12a. The structure consists of a porous silicon ridge waveguide perforated with a series of linear holes designed specifically to create two mirror regions with a cavity region in between. Electron beam lithography and

reactive ion etching were carried out to fabricate the structure. The molecular detection sensitivity of the porous silicon nanobeams was characterized by functionalization with a 16-base DNA molecule for the capture of a 16-base complimentary PNA molecule (Fig. 12b). The detection of target PNA results in a 2 pm/nM sensitivity, which is similar to that of the porous silicon ring resonators and is one order of magnitude improved over SOI nanobeams that have substantially less accessible surface area. A detection sensitivity of 1130 nm/RIU was estimated for the detection of small chemical molecules using the porous silicon nanobeam sensors.

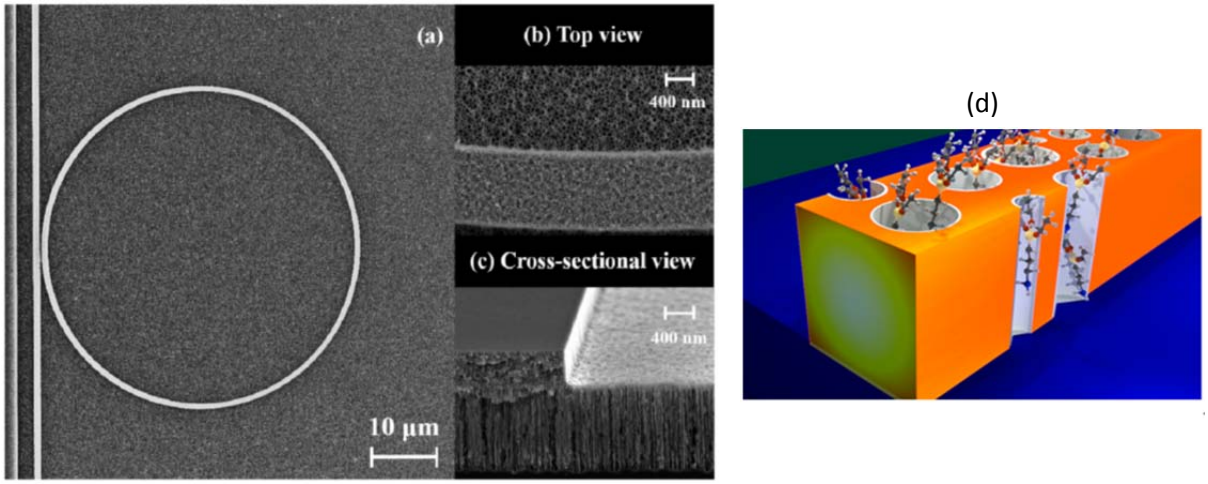

Figure 11. (a) SEM image of a 25µm radius porous silicon ring resonator along with high magnification (b) top and (c) cross-sectional views. (d) Schematic illustration of porous silicon ring waveguide showing that target molecules can access the waveguide center where most of the light is localized. This strong light-molecule interaction improves detection sensitivity. [19]

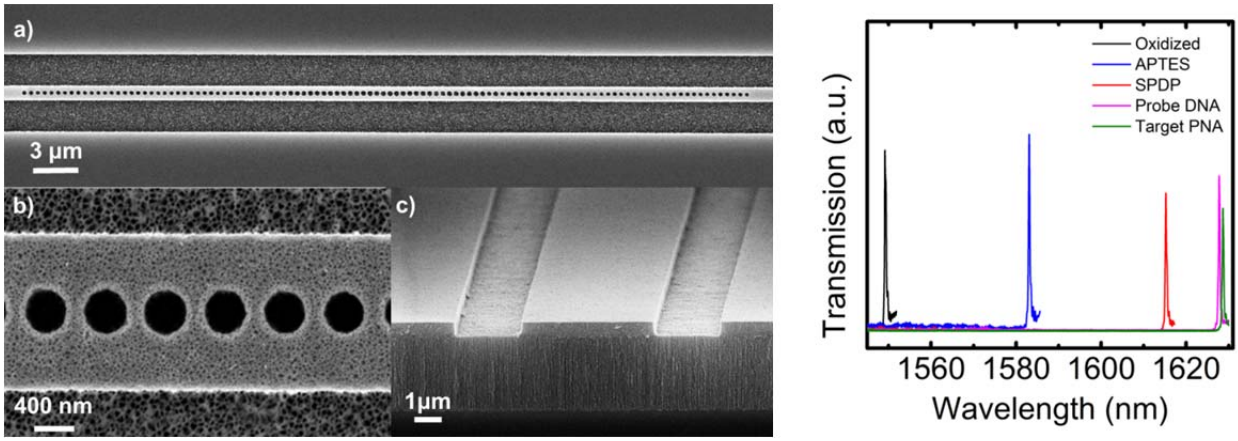

Figure 12. (a) SEM image of porous silicon photonic crystal nanobeam cavity and (b) zoom in of air holes. (c) Cross-sectional SEM image of the coupling ridge waveguide. (d) Transmission spectra of porous silicon nanobeam resonances showing the detection of small chemical linker molecules (APTES and SPDP), probe DNA, and target PNA. [20]

(10) Fabrication of robust porous silicon membranes that allow evaluation of infiltration and binding kinetics in open-ended porous media

Most sensors based on porous materials utilize a flow-over regime in which the fluid containing the analyte of interest is transported over the porous surface. In this case, since nanoscale pores tend to have very high aspect ratios, the analyte delivery is almost exclusively governed by diffusion. Hence, the performance of porous sensors is traditionally limited by slow response times. In order to investigate methods of improving analyte transport, we developed a technique based on standard lithographic techniques to fabricate open-ended porous silicon membranes [21]. The porous silicon film was first formed by electrochemical etching and then electron beam lithography and two aligned reactive ion etch steps were used to open up the membranes. Figure 13a shows a schematic comparison of the flow-over and flow-through approaches to molecular detection with porous sensors and Fig. 13b shows images of the porous silicon membrane. In this work, a porous silicon microcavity was formed with sacrificial layers on the top and bottom to provide fabrication tolerance during reactive ion etching. The microcavity structure provides a resonant feature in the reflectance spectrum that can be tracked in real time to help determine kinetic parameters of molecules in the pores.

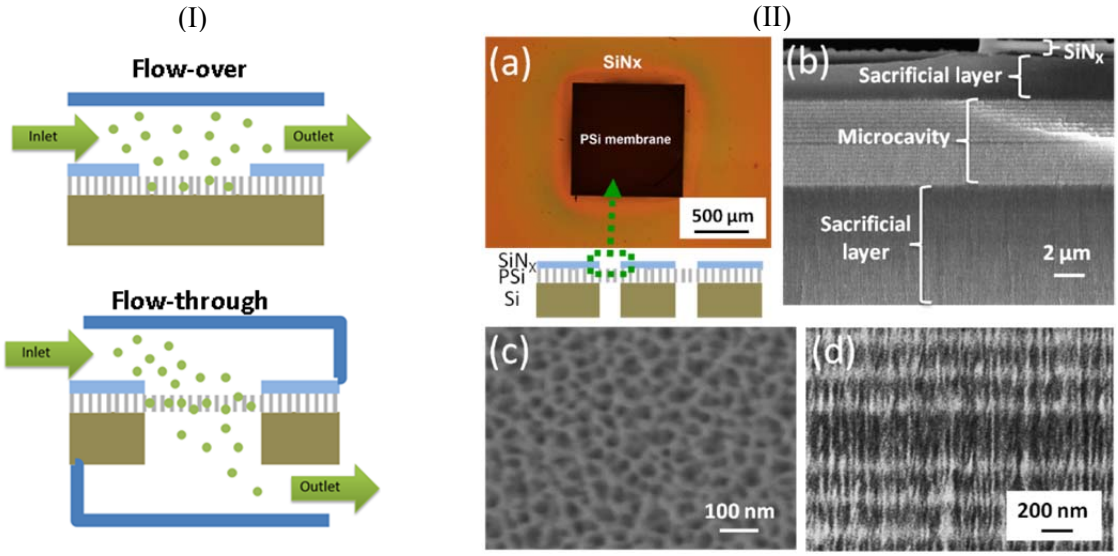

Figure 13. (I) Schematics of flow-over (upper) and flow-through (lower) porous sensors. Improved infiltration and binding kinetics can be achieved using open-ended pores in the flow-through design. (II) (a) Optical microscope image and schematic illustration of porous silicon membrane surrounded by silicon nitride. (b) Cross-sectional SEM image of the edge of the membrane region showing the sacrificial layers, porous silicon layers comprising the microcavity, and the remaining silicon nitride film. (c) Top view SEM image of the porous silicon membrane region. (d) Magnified cross-sectional SEM image of the microcavity region showing the high quality of the interfaces. [21]

To facilitate real-time biosensing measurements using the porous silicon membrane platform, polydimethylsiloxane (PDMS) microfluidic flow cells were attached. On-substrate porous silicon microcavities with the same sacrificial layers were also fabricated with PDMS

flow cells for comparison studies. The porous silicon sensors were first functionalized with 2% 3-aminopropyltriethoxsilane (3-APTES, 0.8 nm) solution in water and methanol, and 1 mM sulfo-NHS-biotin (1 nm) diluted in water. Various concentrations of the protein molecule, streptavidin (STV, 52.8 kDa, 5 nm), were then continuously flowed at 2 µL/min followed by a rinsing step while measuring the reflectance signal from the sensor. When the STV binds to the biotin-functionalized pore walls, the effective refractive index of the porous silicon increases, which causes a red-shift of the microcavity resonance wavelength. Figure 14a shows the comparison of the real-time response of the flow-through and flow-over porous silicon microcavity sensors upon exposure to STV, demonstrating the decreased response time of the membrane structure. Using the porous silicon microcavity membrane flow-through scheme, saturation of the binding sites was achieved within approximately 25 minutes while it took more than 2 hours for the porous silicon microcavity in the flow-over scheme to saturate. Figure 14b reveals the improved sensitivity of the flow-through scheme when the resonance shift of the porous silicon microcavity sensors is measured at the 20 minute time point; the resonance shift is approximately 5 times larger for sensors in the flow-through scheme. Only for long incubation times and high target molecule concentrations does the performance of on-substrate porous silicon sensors approach that of the porous silicon membranes. These results show that the open-ended porous silicon membranes enable effective and efficient analyte delivery and reduce the sensor response time for STV detection. Follow-on computations further elucidated the inverse scaling of response time improvement with molecular diffusivity [21].

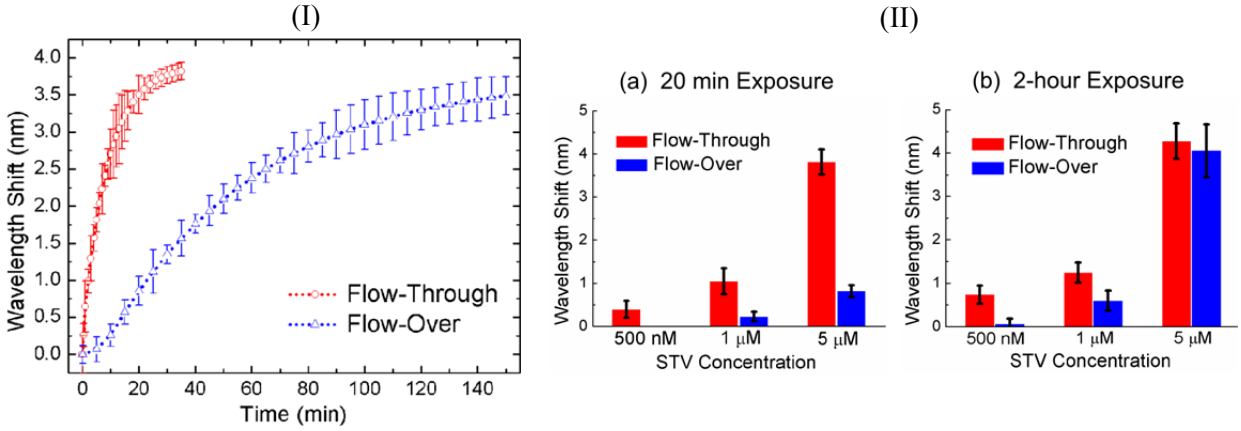

Figure 14. (I) Comparison of real-time porous silicon sensor response to 5 µM streptavidin solution with different flow schemes: flow-through microcavity membranes and flow-over on-substrate microcavity sensors. Measured porous silicon microcavity resonance wavelength shifts were plotted as a function of exposure time. (II) Porous silicon microcavity wavelength shift measured after (a) 20 min and (b) 2 h exposures to 500 nM, 1 µM, and 5 µM streptavidin solutions under the different flow schemes. [21]

References

[1]X. Wei, J. W. Mares, Y. D. Gao, D. Li, S. M. Weiss, "Biomolecule kinetics measurements in flow cell integrated porous silicon waveguides," Biomed Opt Express **3**, 1993-2003 (2012).

[2]X. Wei, S. M. Weiss, "Guided mode biosensor based on grating coupled porous silicon waveguide," Opt Express **19**, 11330-11339 (2011).

[3]X. Wei, S. M. Weiss, "Grating coupled waveguide biosensor based on porous silicon," Mater. Res. Soc. Symp. Proc. **1301**, 219-224 (2011).

[4]Y. Jiao, D. S. Koktysh, N. Phambu, S. M. Weiss, "Dual-mode sensing platform based on colloidal gold functionalized porous silicon," Appl Phys Lett **97**, 153125 (2010).

[5]J. W. Mares, S. M. Weiss, "Diffusion dynamics of small molecules from mesoporous silicon films by real-time optical interferometry," Appl Optics **50**, 5329-5337 (2011).

[6]J. D. Ryckman, M. Liscidini, J. E. Sipe, S. M. Weiss, "Direct imprinting of porous substrates: A rapid and low-cost approach for patterning porous nanomaterials," Nano Lett **11**, 1857-1862 (2011).

[7]J. D. Ryckman, Y. Jiao, S. M. Weiss, "Three-dimensional patterning and morphological control of porous nanomaterials by gray-scale direct imprinting," Sci Rep **3**, 1502 (2013).

[8]J. D. Ryckman, M. Liscidini, J. E. Sipe, S. M. Weiss, "Porous silicon structures for low-cost diffraction-based biosensing," Appl Phys Lett **96**, 171103 (2010).

[9]Y. Jiao, J. D. Ryckman, P. N. Ciesielski, C. A. Escobar, G. K. Jennings, S. M. Weiss, "Patterned nanoporous gold as an effective SERS template," Nanotechnology **22**, 295302 (2011).

[10]Y. Jiao, J. D. Ryckman, D. S. Koktysh, S. M. Weiss, "Controlling surface enhanced Raman scattering using grating-type patterned nanoporous gold substrates," Opt Mater Express **3**, 1137-1148 (2013).

[11]J. L. Lawrie, *In situ DNA synthesis in porous silicon for biosensing applications*, (Vanderbilt University 2012).

[12]Y. L. Zhao, J. L. Lawrie, K. R. Beavers, P. E. Laibinis, S. M. Weiss, "Effect of DNA-induced corrosion on passivated porous silicon biosensors," ACS Applied Materials & Interfaces **6**, 13510-13519 (2014).

[13]Y. Zhao, J. L. Lawrie, P. E. Laibinis, S. M. Weiss, "Understanding and mitigating DNA induced corrosion in porous silicon based biosensors," Proc. of SPIE **8933**, 893302 (2014).

[14]K. R. Beavers, J. W. Mares, C. M. Swartz, Y. L. Zhao, S. M. Weiss, C. L. Duvall, "In situ synthesis of peptide nucleic acids in porous silicon for drug delivery and biosensing," Bioconjugate Chem **25**, 1192-1197 (2014).

[15]G. A. Rodriguez, J. D. Ryckman, Y. Jiao, S. M. Weiss, "A size selective porous silicon grating-coupled Bloch surface and sub-surface wave biosensor," Biosens Bioelectron **53**, 486-493 (2014).

[16]G. A. Rodriguez, J. D. Lonai, R. L. Mernaugh, S. M. Weiss, "Porous silicon Bloch surface and sub-surface wave structure for simultaneous detection of small and large molecules," Nanoscale Res Lett **9**, 383 (2014).

[17]G. A. Rodriguez, J. D. Ryckman, Y. Jiao, R. L. Fuller, S. M. Weiss, "Real-time detection of small and large molecules using a porous silicon grating-coupled Bloch surface wave label-free biosensor " Proc. of SPIE **8570**, 857004 (2013).

[18]G. Gaur, D. S. Koktysh, S. M. Weiss, "Immobilization of quantum dots in nanostructured porous silicon films: characterizations and signal amplification for dual-mode optical biosensing," Adv Funct Mater **23**, 3604-3614 (2013).
[19]G. A. Rodriguez, S. R. Hu, S. M. Weiss, "Porous silicon ring resonator for compact, high sensitivity biosensing applications," Opt Express **23**, 7111-7119 (2015).
[20]G. A. Rodriguez, P. Markov, A. P. Cartwright, S. T. Retterer, I. I. Kravchenko, S. M. Weiss, "Photonic crystal nanobeam biosensors based on porous silicon," Manuscript in preparation.
[21]Y. Zhao, G. Gaur, S. T. Retterer, P. E. Laibinis, S. M. Weiss, "Flow-through porous silicon membranes for real-time label-free biosensing," in review.